

CVaR in G-VAR : Financial Markets Vulnerabilities and Left-Tail Risk Spillovers

Ahmed-Amine EL AZDI

Université Paris Dauphine - PSL

Abstract

This paper proposes an empirical framework to assess the *ad-hoc* tail risk connectedness across financial markets. I discuss the role of systemic risk as a predictor of financial tail risks in the quantile regression framework introduced in [Adrian et al. \(2019\)](#). I independently estimate the expected shortfall, also called conditional value-at-risk (CVaR), for four asset classes. Surprisingly, systemic stress has little informational power over future tail outcomes in those asset classes, even if the overall picture is not homogeneous across markets. The CVaR measures constructed as the tails of predictive conditional distributions are then taken to a generalized vector autoregression (G-VAR) framework in which forecast-error variance decompositions are invariant to the variable ordering as in [Diebold & Yilmaz \(2012\)](#) to build a directional left-tail risk spillovers measure. I find strong evidence of high dependence between the tails of the distributions across financial markets with risks of contagion during episodes of high volatility.

Keywords: Expected shortfall, asset returns, quantile regression, systemic risk, tail risk spillovers, tail dependence, G-VAR

1 Introduction

In the realm of financial economics, understanding and managing market risks is paramount, not just for academic inquiry but for safeguarding the pillars of global economic stability and financial integrity. Episodes of pronounced volatility, catalyzed by a spectrum of triggers from macroeconomic shifts to global health emergencies, pose intricate challenges to policymakers, financial analysts, and scholars alike. These episodes are not merely statistical outliers; they are pivotal events that shape the risk landscape of financial markets, influencing asset valuations and investment strategies fundamentally.

The theoretical framework established by [Rietz \(1988\)](#), further explored and supported by [Barro \(2006\)](#), and empirically substantiated by [Gabaix \(2012\)](#), positions rare, catastrophic events as central to understanding asset risk premia. This body of work argues convincingly that disasters—economic depressions, wars, and pandemics—while seemingly infrequent, have occurred with enough regularity and severity to significantly influence the equity market’s risk premium. These insights pivot on the notion that asset values and, consequently, risk premiums are not static but fluctuate over time, influenced heavily by extreme market events.

The scholarly pursuit to decode and model the impacts of extreme financial and economic risks has yielded a vast and varied literature. [Tsai & Wachter \(2015\)](#) provide an extensive survey of this intellectual terrain, navigating through models of disaster risk and fat tails that attempt to unravel the complexities underlying several asset pricing puzzles. The challenge, as illuminated by these studies, lies not just in forecasting these extreme tail risks but in developing robust models that accurately encapsulate the multifaceted nature of financial markets, thereby enabling a nuanced understanding and management of risk spillovers across different market segments.

This paper endeavors to weave together two distinct yet critical strands of literature within financial economics: the Market Risk Approach and the Tail Risk Approach. Historically, these bodies of work have progressed along parallel tracks—the Market Risk Approach, rooted in the diversification theory pioneered by [Markowitz \(1952\)](#) and expanded upon through dynamic models like GARCH of [Engle \(1982\)](#),

offers insights into the evolving nature of market risks. Conversely, the Tail Risk Approach delves into the realms of contagion, extreme value theory, and the dynamic modeling of tail risks, as seen in the multivariate extensions of CAViaR (White, Kim, and Manganeli, 2015) and the $\Delta CoVaR$ measure of Adrian & Brunnermeier (2016).

In bridging these two significant but so far largely separate bodies of literature, this paper introduces a novel conceptual framework: a dynamic measure of left-tail spillovers. This measure not only seeks to illuminate the connectedness and the multifaceted nature of extreme market risks but also offers a groundbreaking perspective on understanding and managing the systemic vulnerabilities inherent in financial markets. The introduction of this dynamic left-tail spillovers measure is poised to transform how we conceptualize the propagation of risks across different asset classes, providing a more granular and dynamic understanding of risk interdependencies.

Our contribution to the literature is multifold. We extend the dialogue on tail risks and their broader macroeconomic implications, particularly engaging with the Growth-at-Risk (GaR) paradigm as conceptualized by Adrian et al. (2019). This framework, which has been instrumental in linking financial conditions to economic growth projections, employs the Conditional Value-at-Risk (CVaR) concept in a novel manner, allowing for a comprehensive assessment of potential economic downturns based on prevailing financial conditions. By integrating the VaR concept and its extensions, such as the Conditional Autoregressive Value-at-Risk (CAViaR) model, into our analysis, we aim to offer new insights into the conditional dynamics of risk and the complex interplay between financial markets and macroeconomic stability.

Building upon this framework, a lot of papers have been using the same methodology to assess risks to economic activity over time on other economic aggregates (e.g. GDP-at-risk in Aikman et al. (2019) and inflation-at-risk in López-Salido & Loria (2020)). Those so-called "*X-at-Risk*" models, for X being any economic or financial variable, are heavily relying on the Value-at-Risk (VaR) concept in portfolio management and finance. They are fundamentally different from the point forecast models, because in the "*X-at-Risk*" models the prediction is a hole distribution that allows the econometrician to consider the risks around his forecasts. Furthermore, they are using an augmented version of the VaR model called CAViaR for Conditional Autoregressive Value-at-Risk model as developed in Engle & Manganeli (1999) to capture the time variation of the quantile and estimate the parameters with regression quantiles.

All this previous work has been using the same specification *i.e.* financial conditions as a driver of macroeconomic vulnerabilities and quantile regressions (QR) as a tool to capture the nonlinearities between financial and economic variables. Some other papers departed from this specification and use indicators of systemic stress as the CISS introduced in Kremer et al. (2012) to measure financial conditions, as in Ferrara et al. (2020) and Figueres & Jarociński (2020). The latest focused on the performances of different measures of financial conditions and showed that for the euro area the CISS is more informative than indicators that focus on specific segments of financial markets or even using their simple aggregation in the principal component. Other papers like Caldara et al. (2022) used Markov-switching process instead of QR to capture the non-linear responses of growth to financial conditions. They also manage to show that tighter financial conditions dramatically increase the probability of tail risks of large negative growth.

Our methodological approach distinguishes itself through a two-stage procedure that meticulously estimates the conditional and unconditional predictive densities for key financial asset classes. This nuanced approach allows us to explore the limits of systemic risk indicators' predictive capabilities and to uncover the intricate web of tail risk connectedness across financial markets. Our findings highlight the critical role of tail risk spillovers, particularly those originating from equity markets, underscoring the need for sophisticated models that account for the cross-correlation of tails in comprehensive risk assessments.

The first stage uses the framework introduced in Adrian et al. (2019) to estimate the conditional and unconditional predictive densities of four financial asset classes, which are the equity, fixed income, commodities and foreign exchange markets. This is achieved by smoothing the quantile regression functions of Koenker & Bassett (1978) using the flexible probability density distribution of Azzalini & Capitanio (2003). Consequently, we generate a time series of vulnerability for each of the considered financial markets that we call respectively Equity-at-Risk (EaR), Fixed income-at-Risk (FIaR), Foreign exchange-at-

Risk (FX-at-Risk) and Commodity-at-Risk (CaR). Then, we back-test the estimated predictive densities as done in Rossi & Sekhposyan (2014) by analysing the predictive score and the probability integral transform (PIT).

In the second stage, we use the generalised vector autoregression framework of Koop et al. (1996) and Pesaran & Shin (1998) in which forecast-error variance decompositions are invariant to the variable ordering. In this framework, we build a directional left-tail risk spillovers measure as in Diebold & Yilmaz (2012).

The first step provides indications that systemic risk is not a strong predictor of future tail outcomes in financial markets. However, both the conditional and unconditional estimated densities display very strong out-of-sample performance. The second stage brings to light the tail connectedness across financial asset classes and the sizable amounts of tail risk spillovers across markets. This two-stage procedure provides strong empirical evidence of high contagion risk across financial markets due to their tail dependence. Especially tail risk spillovers going from the market for equities to the others. Indeed, we find spillovers across tails that are three times bigger than the total spillover index found in Diebold & Yilmaz (2012), which shows that tail risk spillovers are higher than gross return spillovers. This calls for a methodology taking into account the cross-correlation of the tails. Manganelli et al. (2015) provides a multi-variate, multi-quantile model that goes a step in this direction.

I proceed as follows. In section 2 I discuss the potential nonlinear relationship between systemic stress and financial markets. In section 3 I build the predictive densities of each of those financial asset classes. Section 4 describes the methodology to build vulnerability measures and describes its results. In section 5 I evaluate and discuss left-tail risk spillovers. Section 6 concludes.

2 Financial Markets and Systemic Stress

To evaluate the rigidity and tightness of financial conditions, I use systemic risk and the Composite Indicator of Systemic Stress (CISS)¹. The CISS is a weekly-specific statistical design built around the common definition of systemic risk as the aggregation of five market-specific indices. Those indices are created from a total of 15 individual financial stress measures, which are aggregated using basic portfolio theory. Kremer et al. (2012) describes the methodology for the CISS, which is based on the aggregation of those financial stress measures and taking into account the time-varying cross-correlations between these measures. The data for the Yield curve spot rate at 10-year maturity starts in January 2005, this will be the starting time for my empirical work.

To describe conditions in financial markets, I adopt the same approach as Diebold & Yilmaz (2012) where I consider four main categories of financial markets which are the equity market (measured by the Euronext 100²), the fixed income market (measured by the 10-year bond yield³), the market for commodities (measured by the ECB Commodity Price Index⁴) and the foreign exchange market (measured by the Euro/Dollar exchange rate⁵). This dichotomous approach allows us to get a better picture of the relationships between each financial segment and the level of systemic stress.

To characterise this relationship, I choose to focus on the returns of those financial segments. Usually, most of the literature on financial analysis and risk management uses the Rate of Return (RoR) as a measure of returns. Here, this kind of measure will not yield consistent time series to conduct my analysis. The reason is the different nature of the data chosen for this work. Indeed, the financial data I use is available on the ECB Statistical Data Warehouse and I use those financial time series to compute the returns on each asset class. The issue that arises is that the RoR provides a time series that is not stationary for the fixed income market. This is due to the fact that the bond yield reaches the zero lower bound (ZLB) around 2015. This makes the denominator close to zero when we are calculating returns

¹https://sdw.ecb.europa.eu/quickview.do?SERIES_KEY=290.CISS.D.U2.Z0Z.4F.EC.SS.CI.IDX

²Data for the Euronext 100 is taken from Yahoo Finance data

³https://sdw.ecb.europa.eu/quickview.do?SERIES_KEY=165.YC.B.U2.EUR.4F.G.N.A.SV.C.YM.SR.10Y

⁴https://sdw.ecb.europa.eu/quickview.do;jsessionid=FOEDD2F3CAB12FB9FC562D07ED3F687F?SERIES_KEY=132.STS.M.I8.N.UWIE.CTOTNE.3.000

⁵https://sdw.ecb.europa.eu/quickview.do?SERIES_KEY=120.EXR.D.USD.EUR.SP00.A

based on the RoR, which yields a non-stationary time series. This will *a posteriori* yield vulnerability measures that are not consistent.

In an effort to get rid of this issue, I use a standardised first difference as a proxy for the period-to-period returns on each asset class. Let V_t be the market value at time t of a financial asset class X . The standardised first difference of the asset class X is noted as r_t^X which is defined as :

$$r_t^X = \frac{V_t^X - V_{t-1}^X}{\sigma_{t-1}^X}$$

I use this measure to compute the returns on each asset class. It provides stationary time series that can be used to conduct our empirical investigation. *Figure 1* displays the four resulting time series against the CISS. This figure gives the first indication of the absence of a clear linear relationship between the asset returns on all four classes and the CISS. However, for the equity market and foreign exchange markets, it seems that periods of high volatility coincide almost at the same time with spikes on the CISS. Other than that, those time series do not display any obvious pattern or correlation between financial asset returns and the level of systemic risk.

It is important to note that financial asset returns are much more volatile than the CISS. Plus, the equity market display some evidence that extreme negative returns occur roughly at the same time as high outcomes of the CISS, especially during the 2007 subprime crisis, the 2012 European sovereign debt crisis and the early stages of the COVID-19 pandemic in 2020. On the other hand, the bond, commodities and foreign exchange markets do not show an obvious similar pattern. Those three time series are very erratic and show levels of volatility that are almost constant over time.

Our objective here is to investigate which one (if any) of these financial asset returns features a non-linear relationship with the level of systemic stress. There are several methods we can use to capture the non-linear links between our financial variables and financial condition indices. We choose quantile regression (QR) to identify formally the relationship between our financial variables and the current level of financial markets systemic stress.

Let's denote r_{t+h}^X the monthly return on a financial asset class X calculated as a standardised first difference between t and $t+h$, then x_t is the vector that contains a constant and the conditioning variables. Thus, the coefficient $\hat{\beta}_\tau$ of the quantile regression of r_{t+h}^X on x_t is given by:

$$\hat{\beta}^X(\tau) = \underset{\beta_\tau \in \mathbb{R}^k}{\operatorname{argmin}} \sum_{t=1}^{T-h} \left(\tau \cdot \mathbb{1}_{(r_{t+h}^X \geq x_t \beta)} |r_{t+h}^X - x_t \beta_\tau| + (1 - \tau) \cdot \mathbb{1}_{(r_{t+h}^X < x_t \beta)} |r_{t+h}^X - x_t \beta_\tau| \right)$$

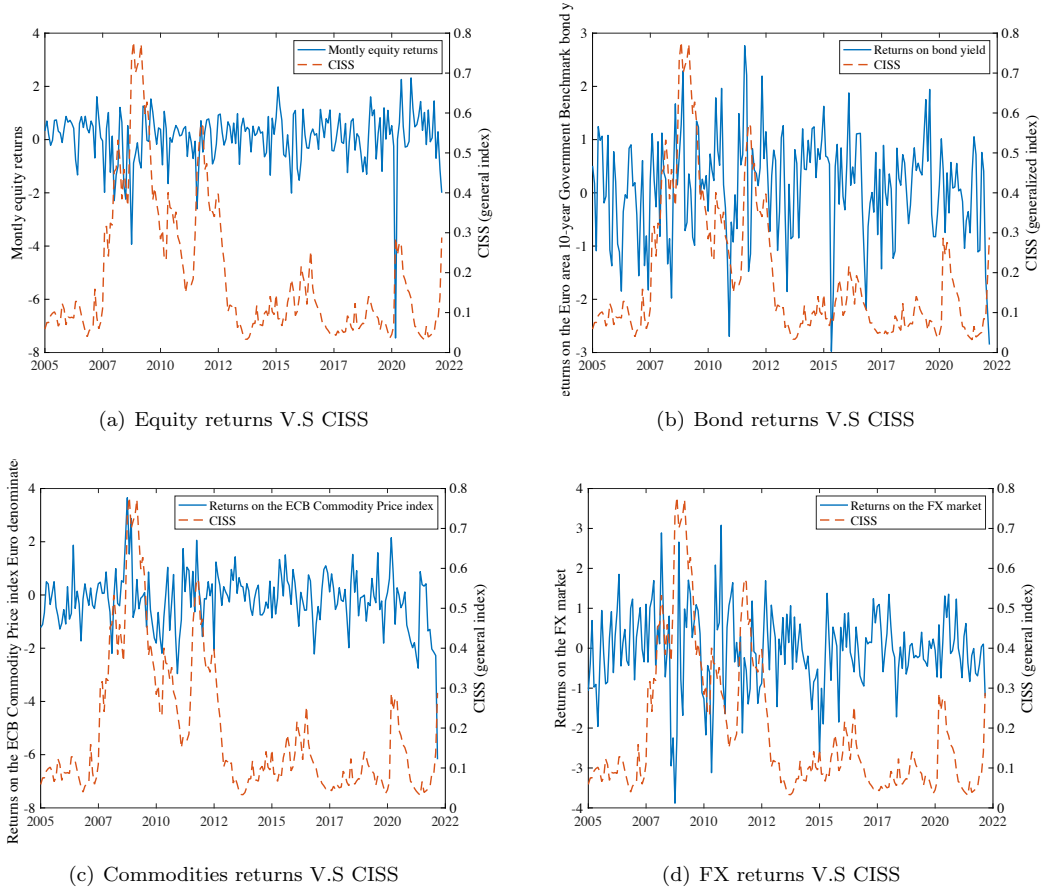
With $\mathbb{1}_{(\cdot)}$ the indicator function.

$$\hat{Q}_{r_{t+h}^X | x_t}(\tau | x_t) = \hat{\beta}^X(\tau)' x_t$$

Knowing that the $\hat{Q}_{r_{t+h}^X | x_t}(\tau | x_t)$ is a consistent linear estimator of conditional quantile function (see [Koenker & Bassett \(1978\)](#)). We can see two main differences between a quantile regression and a standard OLS regression. The first one is that QR minimise the absolute errors while the OLS minimise the squared errors. The second difference is that QR assign different penalties τ and $1 - \tau$ if the predictor $\hat{\beta}^X(\tau)' x_t$ is respectively, above or below the true value r_{t+h}^X .

Figure 2 is a scatter plot of the one-month-ahead standardised first difference of each asset class against the current asset class returns and the current CISS (panels (a) and (b)). The green, red and dark lines refer to the 5th, 50th and 95th quantiles of the univariate QR respectively, while the blue solid line refers to the OLS regression line. The first thing we notice is that the four asset classes do not display the same features.

Figure 1: Raw Data for all considered Markets



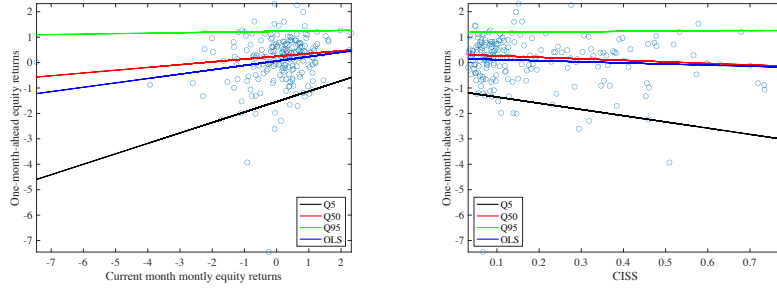
Remarks: This figure displays the standardised first difference of each asset class against the CISS.

We can easily see in panel (a) that the one-month-ahead stock returns have a steep positively sloped 5^{th} quantile regression line, while the 95^{th} QR line is almost flat for this asset class. The OLS and the 50^{th} QR line are almost the same gradual positively sloped line. On the other hand, panel (b) shows that CISS features a negatively sloped 5^{th} quantile regression line, while the 50^{th} 95^{th} QR lines and the OLS regression line are almost flat.

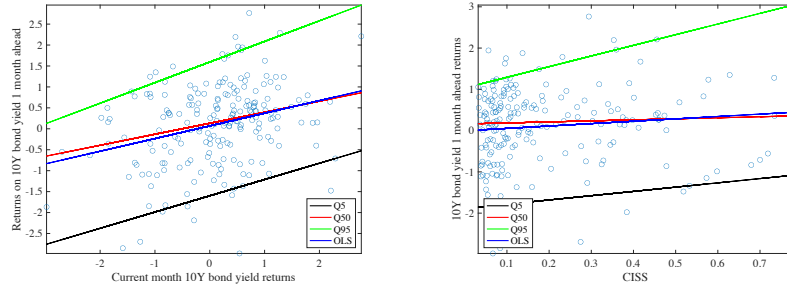
Then, panels (c),(e) and (g) show a similar picture. Here, we have the bonds, Commodities and FX market returns respectively regressed on their lagged values. The panels show steep positively sloped OLS and QR lines. Those slopes are almost the same for each asset class with parallel regression lines. Then, panels (d) and (f) show the OLS and univariate regression of the current asset class returns (here it is the bond and commodities markets) on the CISS. Those two panels show that for the CISS, the slopes do not differ significantly across quantiles and from the linear regression line. This is our first evidence that those markets do not feature a nonlinear relationship between them and the level of systemic stress in the economy. Finally, panel (h) shows that the regression slope changes drastically for the CISS across quantiles. This shows that the CISS will have great informational power to predict tail outcomes for the foreign exchange market.

Figure 3 shows the one-month-ahead estimated coefficients of the quantile regressions when both the current asset class returns and the CISS are included in the regression. We notice that our four asset classes do not feature the same properties with respect to the coefficients corresponding to the CISS. The FX market has CISS coefficients that vary drastically across quantiles, which is consistent with the results found in panel (h) of Figure 2. It means that the systemic stress has a strong nonlinear relationship with the FX market returns and will have strong informational power on the variations on the downside and upside risks. This goes to show that the CISS coefficients do not change significantly when we add the current FX market asset returns to the quantile regression.

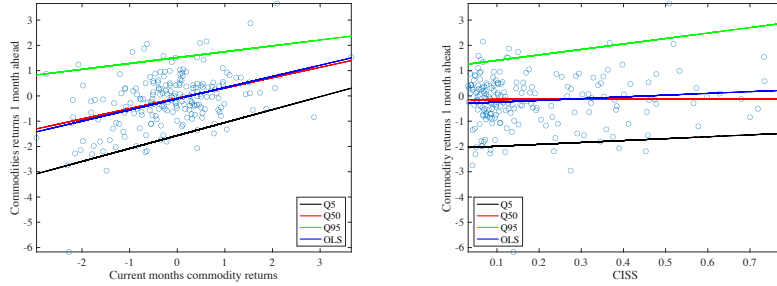
Figure 2: Quantile Regressions



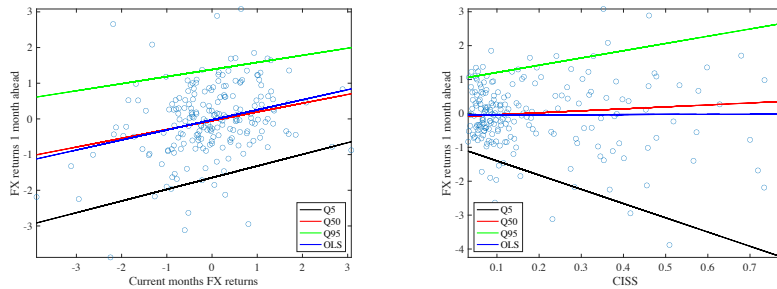
(a) QR of one-month-ahead Equity returns on the current Equity returns (b) QR of one-month-ahead Equity returns on the CISS



(c) QR of one-month-ahead Bond returns on the current Bond returns (d) QR of one-month-ahead Bond returns on the CISS



(e) QR of one-month-ahead Commodities returns on the current Commodities returns (f) QR of one-month-ahead Commodities returns on the CISS



(g) QR of one-month-ahead FX returns on the current FX returns (h) QR of one-month-ahead FX returns on the CISS

Remarks: This figure shows univariate quantile regressions at different quantile thresholds as long as the OLS regression line.

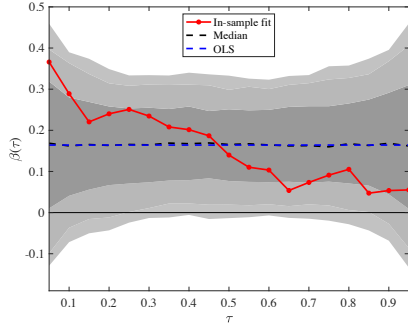
On the other hand, the picture changes for the commodities market where we notice that the coefficients of the CISS start to feature a stronger nonlinear relationship with the commodities returns. Plus, the current commodities market return also features quantile coefficients that vary significantly across quantiles. This feature is shared with the two other asset classes, namely the equity market and the

bonds market, which also shows that when the current asset class returns and the CISS are regressed on the one-month-ahead asset class returns, the CISS will show coefficients that do not differ significantly from the OLS coefficient but the current asset class returns are featuring coefficients across quantiles that differ significantly from the OLS slope. This is an indication that low returns are associated with higher returns on the previous period while the upper quantiles are close to zero, which means that higher returns are not especially correlated with high higher returns on a one-month horizon.

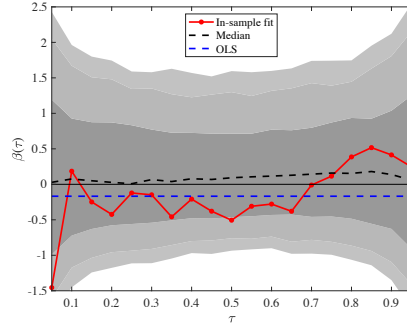
The equity and the bond markets display CISS coefficients that are stable across quantiles and stay close to the OLS slope. This is our first strong evidence that in our case systemic stress does not feature a nonlinear relationship with at least some financial asset classes. Therefore, one could expect the CISS to bring little to no information about tail events. This implies that the variations on the upside and downside risks will not be induced by changes in the level of systemic stress in the economy and will have low predictive power on tail outcomes.

Another surprising result for which we get the initial intuition here is that the quantile regression coefficients are centred around the OLS slope. This goes to show that in some cases and perhaps most of them, the predictive distributions will be symmetrical and centred around the conditional mean. For our analysis, this is a very important result because it is showing that both the upside and the downside risk will vary, which means that both the left tail and the right tail of the predictive distributions change and this yields flatter density functions. Unlike [Adrian et al. \(2019\)](#) where financial conditions display a very strong nonlinear relationship with economic conditions and where only the downside risk matters with upper quantiles that are stable across time.

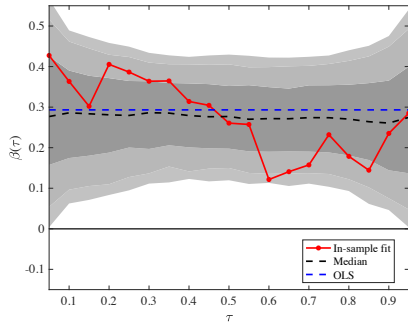
Figure 3: 1-Month-Ahead Estimated QR coefficients



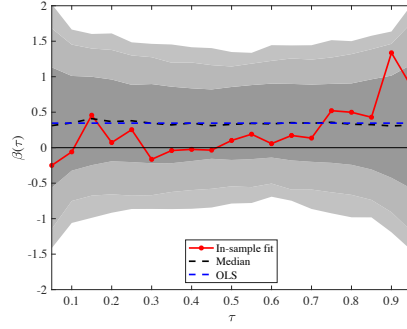
(a) Equity Market Returns



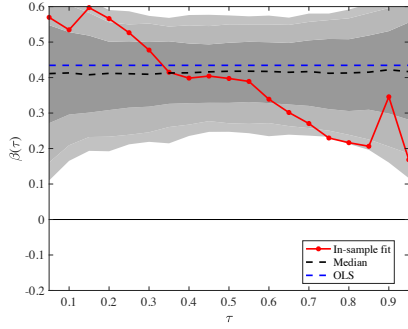
(b) CISS



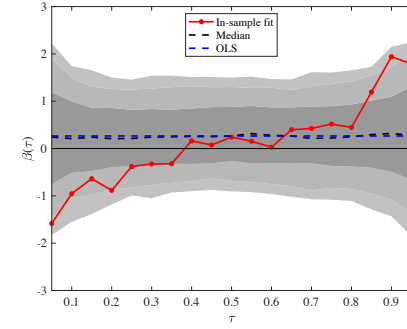
(c) Bonds Market Returns



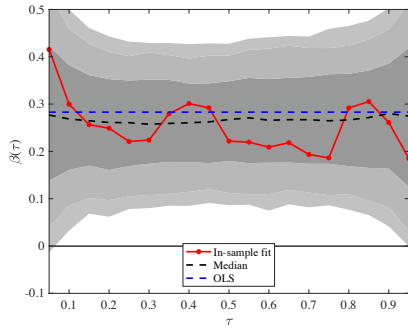
(d) CISS



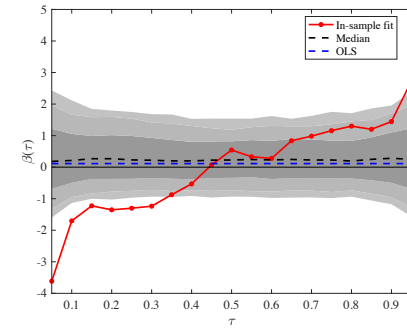
(e) Commodities Market Returns



(f) CISS



(g) FX Market Returns



(h) CISS

Remarks: The above figures are obtained by estimating the coefficients of the regression quantiles of the one-month-ahead asset class returns on the current asset class returns and the current CISS. The grey areas are the confidence intervals for the same null hypothesis as [Adrian et al. \(2019\)](#), that is the true data-generation process is a general, flexible linear model for returns and financial systemic stress (VAR with 4 lags).

3 Building Predictive Distributions

In order to get the predictive distribution, we have to smooth the quantile outputs we get with the quantile functions constructed above. Those quantile functions are to be considered as an inverse cumulative function. To achieve that, we need a flexible parametric distribution that can account for fat tails, asymmetry and flexibility, put in another way, we need to accommodate for high order moments other than just the mean and the variance. The Generalized Skewed-Student density function developed in [Azzalini & Capitanio \(2003\)](#) provides us with a parametric density function that we will use to map the quantile function estimates into a predictive probability density function. The formal definition of this skewed t distribution is the following:

$$f(y; \mu, \sigma, \alpha, \nu) = \frac{2}{\sigma} t\left(\frac{y - \mu}{\sigma}; \nu\right) T\left(\alpha \frac{y - \mu}{\sigma} \sqrt{\frac{\nu + 1}{\nu + \left(\frac{y - \mu}{\sigma}\right)^2}}; \nu + 1\right)$$

where μ : location, σ : scale, ν : fatness and α : shape. And $t(\cdot)$ and $T(\cdot)$ are (pdf) and (cdf) of standard Student distribution. This distribution will be fitted to smooth our quantile function and build our predictive probability density function.

Then, to get our final output we choose for each quantile the parameters of the Generalized Skewed-Student that minimise the quadratic distance between the linear estimator of conditional quantile function $\hat{Q}_{r_{t+h}^X | x_t}(\tau | x_t)$ and the fitted inverse cumulative distribution $F^{-1}(\tau; \mu, \sigma, \alpha, \nu)$. Which can be written as:

$$\{\hat{\mu}_{t+h}, \hat{\sigma}_{t+h}, \hat{\alpha}_{t+h}, \hat{\nu}_{t+h}\} = \underset{\mu, \sigma, \alpha, \nu}{\operatorname{argmin}} \sum_{\tau} \left(\hat{Q}_{r_{t+h}^X | x_t}(\tau | x_t) - F^{-1}(\tau; \mu, \sigma, \alpha, \nu) \right)^2$$

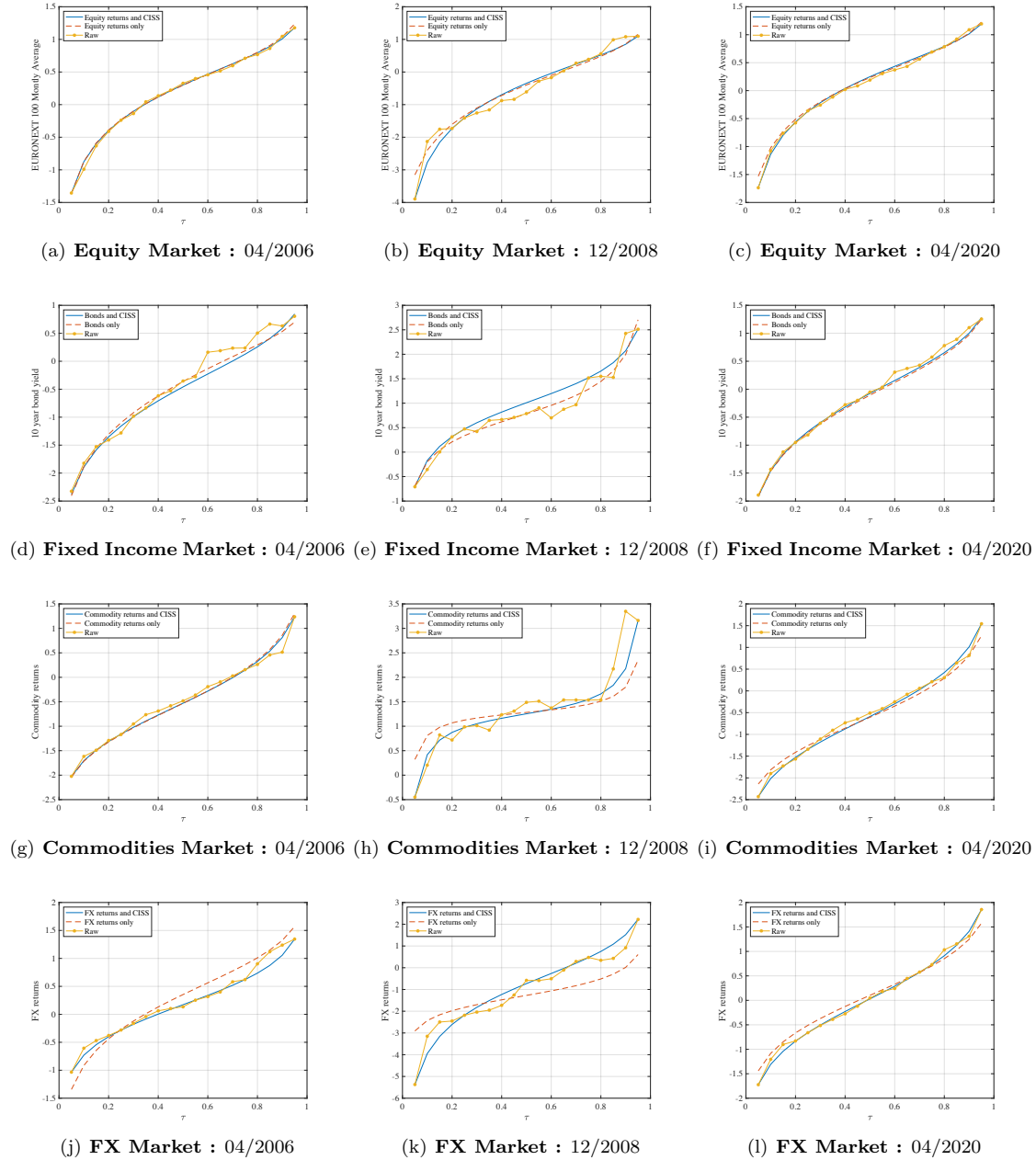
Using both the conditional quantile function *i.e.* $\hat{Q}_{r_{t+h}^X | x_t}(\tau | x_t)$ and unconditional quantile function *i.e.* $\hat{Q}_{r_{t+h}^X}(\tau)$. We get the inverse cumulative distribution $F^{-1}(\tau; \hat{\mu}_{t+h}, \hat{\sigma}_{t+h}, \hat{\alpha}_{t+h}, \hat{\nu}_{t+h})$ for both the conditional and unconditional quantile functions of each asset class. We can then compute the conditional probability density function noted $\hat{f}_{r_{t+h}^X | x_t}(r^X | x_t)$ this distribution is conditional on both the current asset returns and the current level of systemic stress index. Then the unconditional probability density function that we note $\hat{g}_{r_{t+h}^X}(r^X)$ is conditional only the current returns of the asset X , this function is derived by smoothing the estimated unconditional quantiles $\hat{Q}_{r_{t+h}^X}(\tau)$. Those functions are the forecast densities for horizon h and we define them as the following:

$$\hat{f}_{r_{t+h}^X | x_t}(r^X | x_t) = f(r^X; \hat{\mu}_{t+h}, \hat{\sigma}_{t+h}, \hat{\alpha}_{t+h}, \hat{\nu}_{t+h})$$

$$\hat{g}_{r_{t+h}^X}(r^X) = g(r^X; \hat{\mu}_{t+h}, \hat{\sigma}_{t+h}, \hat{\alpha}_{t+h}, \hat{\nu}_{t+h})$$

Figure 4 shows plots of the estimated conditional quantile $\hat{Q}_{r_{t+h}^X}(\tau | x_t)$ which are represented by the yellow starred curve. Those rough quantile curves are being smoothed by the skewed t-distribution. Using the above described method we derive the fitted conditional inverse cumulative skewed t-distribution $F^{-1}(\tau; \hat{\mu}_{t+h}, \hat{\sigma}_{t+h}, \hat{\alpha}_{t+h}, \hat{\nu}_{t+h})$ which is represented by the blue solid curves. Comparably, we get the unconditional fitted conditional inverse cumulative skewed t-distribution by smoothing the unconditional quantile estimates $\hat{Q}_{r_{t+h}^X}(\tau)$ for each asset class X . This figure displays those three functions for three sample periods, the first column is April 2006 which is the middle of the expansion period following the Dot-com bubble burst. Then, the second column of plots is December 2008, which is a couple of months after the bankruptcy of Lehman Brothers during the subprime crisis. Finally, the latter column is April 2020 which corresponds to the first repercussions of the COVID-19 pandemic on European financial markets. This *figure 4* brings evidence that the skewed t-distribution is flexible enough to smooth the given quantile function estimates. Most importantly, the figure shows that both conditional and unconditional are very much the same during the non-crisis period for the four asset classes. However, even during the early stages of the COVID crisis the conditional and unconditional inverse cumulative distributions are overlaid and show no significant difference across all quantiles and for the four asset classes we are considering. While during December 2008 the conclusion is not much different, we notice that the conditional and unconditional inverse cumulative distributions are not significantly different from one another across quantiles. This confirms the intuition we described previously, that the CISS does not bring great information about tail events during crisis periods.

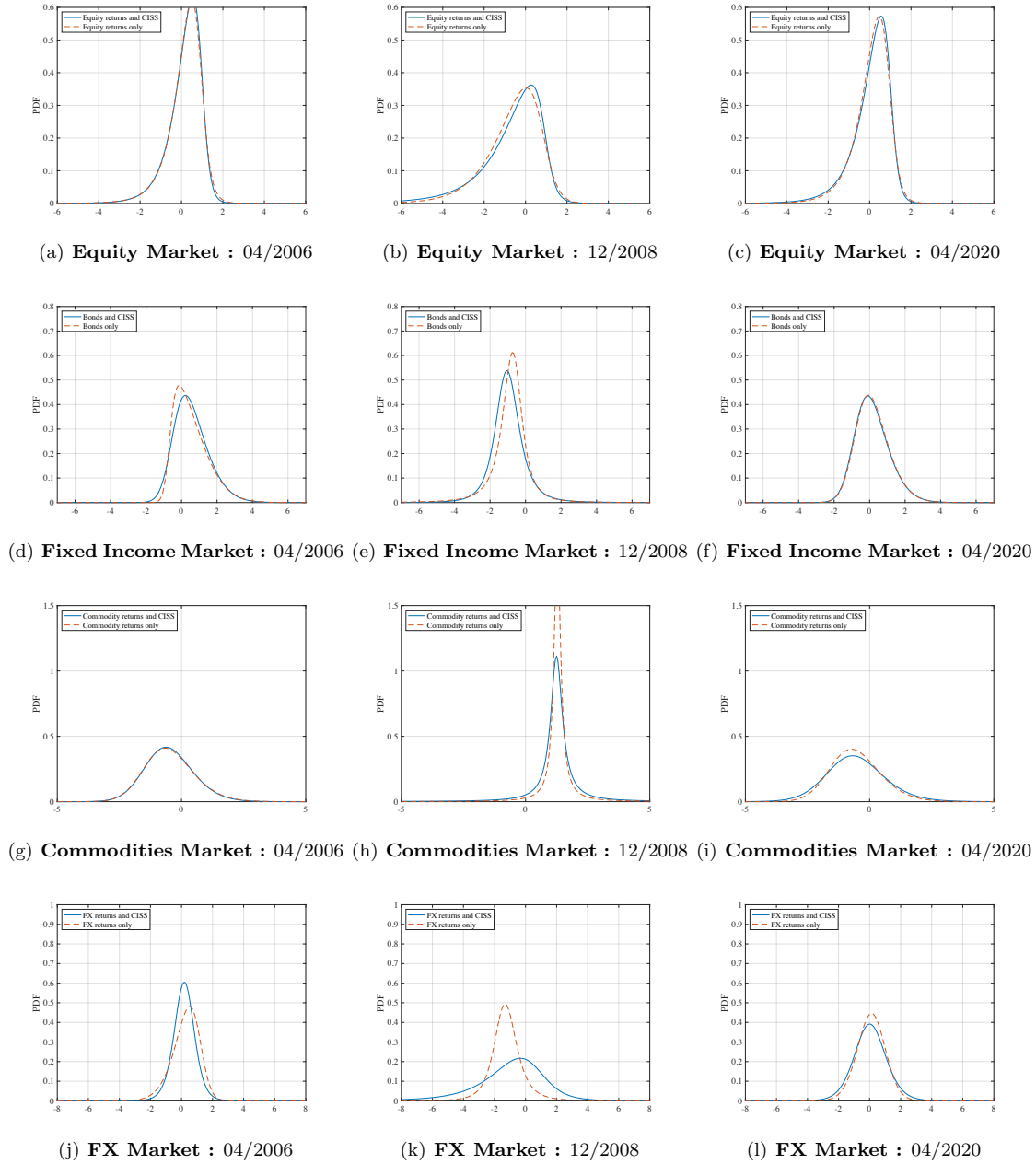
Figure 4: The Conditional and Unconditional Quantiles and the Skewed t-Distribution



Remarks: The panels in this figure show the **conditional quantiles** together with the estimated skewed t-inverse cumulative distribution functions for one-month-ahead asset returns for each class. For comparison, we also report the skewed t-inverse cumulative distribution functions obtained by fitting the **unconditional quantiles** obtained by conditioning only on current asset class return.

To further emphasize these results and observe closely the behaviour of each of these predictive densities we generate *figure 5* that plots the conditional and unconditional probability densities derived using the corresponding estimated inverse cumulative distributions computed above and their estimated parameters $\{\hat{\mu}_{t+h}, \hat{\sigma}_{t+h}, \hat{\alpha}_{t+h}, \hat{\nu}_{t+h}\}$. The figure displays in a similar fashion the same asset classes and sample periods as *figure 4*. This validates our previous conclusion that the conditional predictive probability density functions are not significantly different from the unconditional ones, within and outside of the crisis periods and across all asset classes. The legitimate takeout from this observation is that the CISS bring little to no information about future extreme negative or positive outcomes. There are several explanations for this phenomenon. First, the forecast horizon may be too far and thus financial markets have time to price in the information held by the CISS *i.e.* higher level of systemic risk in the economy.

Figure 5: Conditional and Unconditional Probability Densities



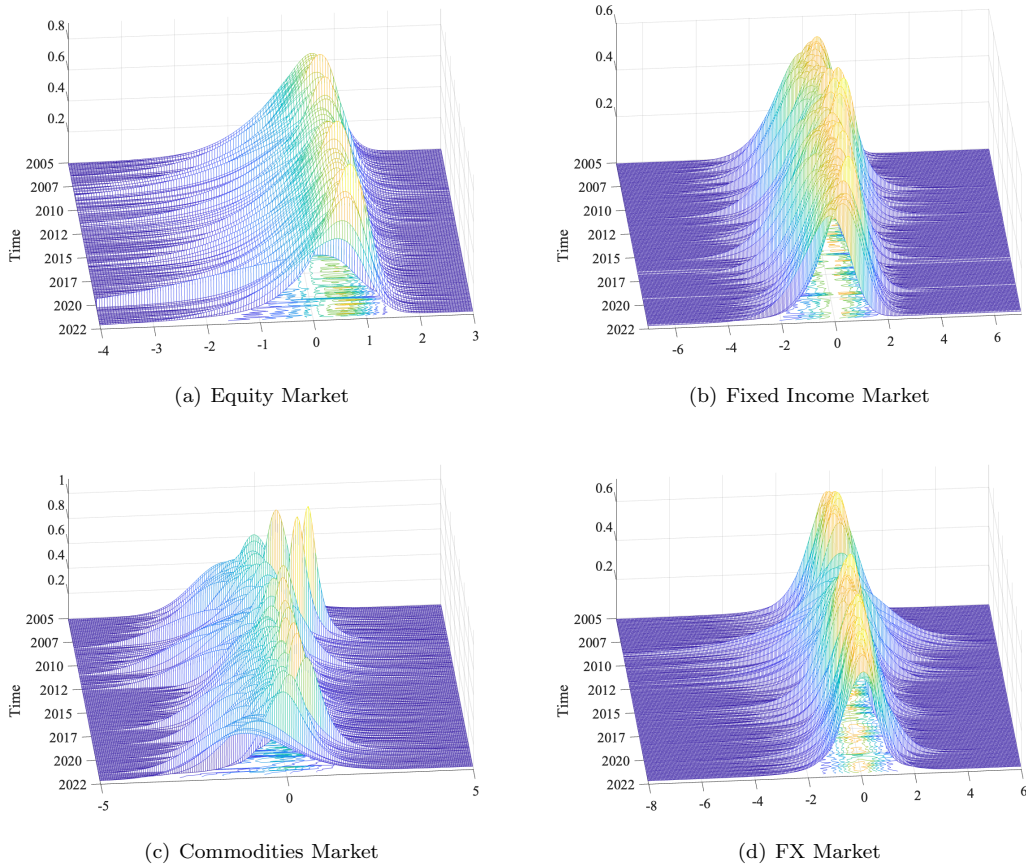
Remarks: The plots displayed in this figure show the unconditional estimated skewed t-density functions for one-month-ahead asset class returns, as long as the conditional density estimated on current asset class returns and the CISS.

Second, the CISS is a measured build as a weighted average of several subindices implied volatility, meaning that the information brought by the CISS is already held by the volatility of the time series we are considering. This result may sound surprising but one can argue that the forecast horizon could be another reason for this. Indeed, we are operating with a one-month-ahead forecast horizon. Given the high-frequency nature of modern financial markets, it is natural to assume that within a one-month horizon, financial markets incorporate all the information provided by systemic risk in the prices. Thus, this result may be sensitive to the prediction horizon and the frequency of the data used. For financial data, it would make more sense to use high-frequency data to capture early signs of financial and systemic stress tightening. However, this is not easy to implement due to the high-frequency nature of financial

variables and the low-frequency nature of systemic risk data. Consequently, the use of mixed frequency data sampling as in Ferrara et al. (2020) could be needed to achieve it.

It is worth noting that papers like Figueres & Jarociński (2020) highlighted the importance of finding the adequate conditioning variable before using this framework. Indeed, they provided evidence that the CISS is the best predictor for tail outcomes of economic growth in the euro area.

Figure 6: Predictive Distribution of Asset Returns over Time



Remarks: This figure shows the one-month-ahead predictive conditional distribution of each asset class returns.

Finally, we plot *figure 6* to show the variations of the conditional predictive distributions across time. We can see that the picture is not homogeneous across financial markets. Indeed, the market for equities shows a stable right side of the distribution, while the left side is very volatile. The FX market in panel (d) shows density functions that get flatter during crisis periods, which translates into higher upside and downside risks. The commodities market in panel (c) displays tails that are very volatile both on the left and right-hand side of the distributions. Finally, the fixed income market in panel (b) shows predictive distributions that are quite stable over time with low tails volatility.

4 Vulnerability Measures

4.1 Information Theory Based Measures

Predicting the downside and upside risks to the forecasts is of paramount importance for investors and risk managers but also policymakers. In this framework, the median of the predicted density provides the modal forecast for the considered asset class returns. This concern is built around the need for better risk assessment around the point forecasts. In other words, how vulnerable the predicted path of returns of a given asset or portfolio is to unexpected shocks and/or unpredictable events.

In this paper, I quantify the upside and downside vulnerability of future asset returns as the net probability that the conditional density allocates to extreme positive and negative tail outcomes. In other words, we compute measures of the disparity between the unconditional density and the conditional density that occurs below the median of the conditional density. By comparing the probability assigned to extreme outcomes by the conditional density to the probability assigned to the same outcomes by the unconditional density, we can assess whether the predicted asset returns distribution in a given period yields greater vulnerabilities around the modal forecast than the unconditional distribution for the corresponding financial market.

Using the same notations as the previous section, we denote $\hat{g}_{r_{t+h}^X}(r^X)$ the unconditional density computed by matching the unconditional empirical quantile functions of each asset class returns and by $\hat{f}_{r_{t+h}^X|x_t}(r^X|x_t) = f(r^X; \hat{\mu}_{t+h}, \hat{\sigma}_{t+h}, \hat{\alpha}_{t+h}, \hat{\nu}_{t+h})$ the estimated conditional skewed t-distribution. We denote the upside relative entropy, \mathcal{L}_t^U , and downside relative entropy, \mathcal{L}_t^D . Those are defined as in [Adrian et al. \(2019\)](#) which means that those measures are the entropy of $\hat{g}_{r_{t+h}^X}(r^X)$ relative to $\hat{f}_{r_{t+h}^X|x_t}(r^X|x_t)$. Formally, those two measures are defined as follows :

$$\mathcal{L}_t^D \left(\hat{f}_{r_{t+h}^X|x_t}(r^X|x_t); \hat{g}_{r_{t+h}^X} \right) = - \int_{-\infty}^{\hat{F}_{r_{t+h}^X}^{-1}(0.5|x_t)} \left(\log \hat{g}_{r_{t+h}^X}(r^X) - \log \hat{f}_{r_{t+h}^X|x_t}(r^X|x_t) \right) \hat{f}_{r_{t+h}^X|x_t}(r^X|x_t) dr^X$$

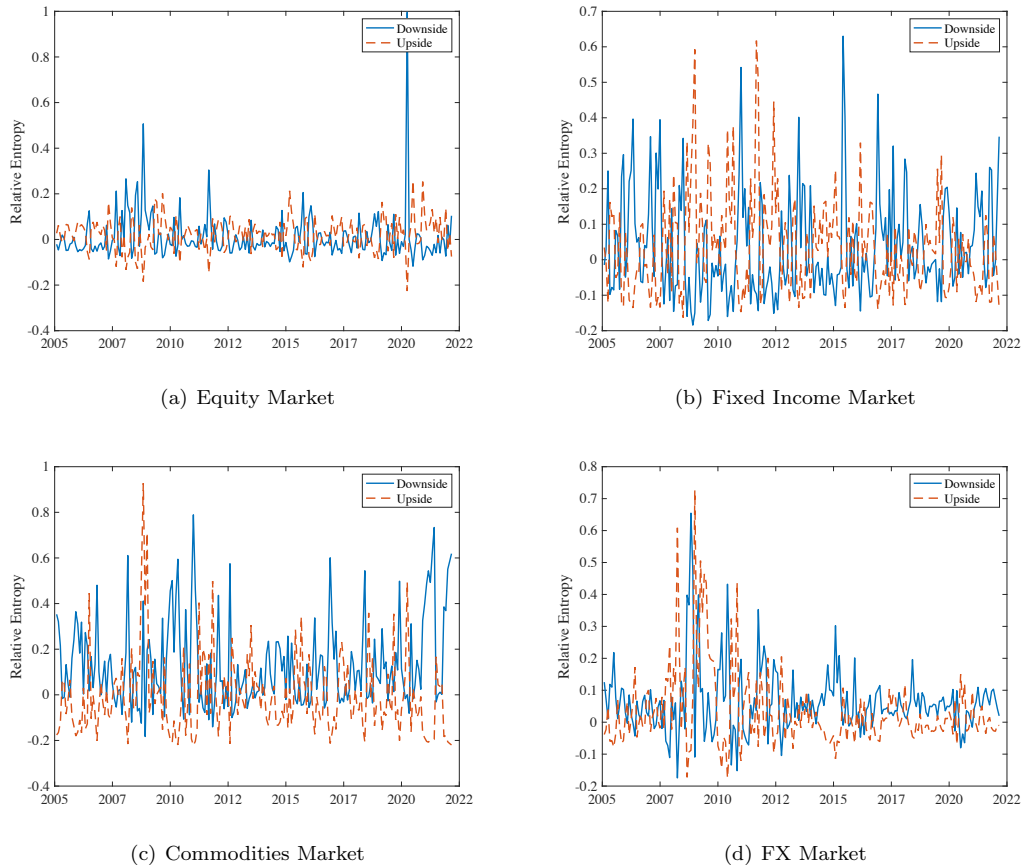
$$\mathcal{L}_t^U \left(\hat{f}_{r_{t+h}^X|x_t}(r^X|x_t); \hat{g}_{r_{t+h}^X} \right) = - \int_{\hat{F}_{r_{t+h}^X}^{-1}(0.5|x_t)}^{\infty} \left(\log \hat{g}_{r_{t+h}^X}(r^X) - \log \hat{f}_{r_{t+h}^X|x_t}(r^X|x_t) \right) \hat{f}_{r_{t+h}^X|x_t}(r^X|x_t) dr^X$$

where $\hat{F}_{r_{t+h}^X}^{-1}(r^X|x_t)$ is the cumulative distribution associated with $\hat{f}_{r_{t+h}^X|x_t}(r^X|x_t)$ and hence $\hat{F}_{r_{t+h}^X}^{-1}(0.5|x_t)$ is the conditional median.

Using the definition given above, we can say that downside entropy measures the discrepancy between the unconditional density and the conditional density that occurs below the median of the conditional density. *Figure 7* plots the upside and downside entropy over time \mathcal{L}_t^U and \mathcal{L}_t^D for each asset class. First looking at downside entropy, by definition the conditional density assigns positive probability to more extreme left tail outcomes or negative returns than the unconditional density when the level of downside entropy is positive and substantial in magnitude. Therefore, panel (a) shows that the equity market displays relative entropy which is close to zero in non-crisis periods and very high relative downside entropy levels during periods of crisis. This implies that the model is very effective at predicting tail events because the conditional density assigns a much greater probability to those events than the unconditional one *i.e.* the CISS brings a great amount of information about future tail outcomes on stock markets. The FX market has a similar feature shown in panel (d) where the relative downside entropy is small in non-crisis periods and increases during periods. We can also see that the entropy goes to the negative territory when the unconditional density assigns a higher probability to tail outcomes than the conditional probability density. For the fixed income and commodities markets, the results discussed in the previous are confirmed. We see in panels (b) and (c) that the downside relative entropy is very erratic and volatile for both markets and does not show a significant difference between crisis and non-crisis periods. This conveys that the CISS does not bring clear information about left tail outcomes due to the noisy feature of those time series. Turning to upside entropy which measures the divergence between the unconditional density and the conditional density that occurs above the median of the conditional density. Upside entropy is represented by the red dashed line in *figure 7* and when it is high, the conditional predictive

probability density allocates a higher probability to extreme right tail events than the unconditional predictive density.

Figure 7: Asset Returns Relative Entropy over Time



Remarks: This figure plots the upside and downside entropy \mathcal{L}_t^U and \mathcal{L}_t^D for each asset class.

Looking at the plotted upside relative entropy the picture changes substantially. We see that for the equity market upside relative entropy is close to zero across time which indicates that the upside risk will be irrelevant for the stock market. Then for the FX market upside, relative entropy comoves with the downside relative entropy which insinuates that the upside risk matter as much as the downside risk for this particular market. Then, the fixed income market in panel (b) shows upside relative entropy that is as chaotic as the downside one, meaning that the CISS does not bring clear information about the right nor left tail events for this particular market. Finally, the commodities market shows downside relative entropy which is less volatile than its downside one and upside entropy which is significantly higher during crisis periods. This evidence suggests that the upside risk matters more than the downside risk for the commodities market and that the CISS could bring valuable and clear informational power about the right tail outcomes for this particular market. This phenomenon could correspond to periods of recovery from the negative shocks endured by the financial markets. It is also clear evidence of the countercyclical feature of the commodities market being a safe haven during times of crisis.

4.2 CVaR Based Measures

In this section, I focus on building a coherent risk measure for the downside risk which is the expected shortfall ES_{t+h} which we also call conditional value-at-risk $CVaR_{t+h}$, then I build its upside equivalent which is called the expected longrise noted EL_{t+h} . For a chosen target probability π , the expected shortfall and longrise are written as :

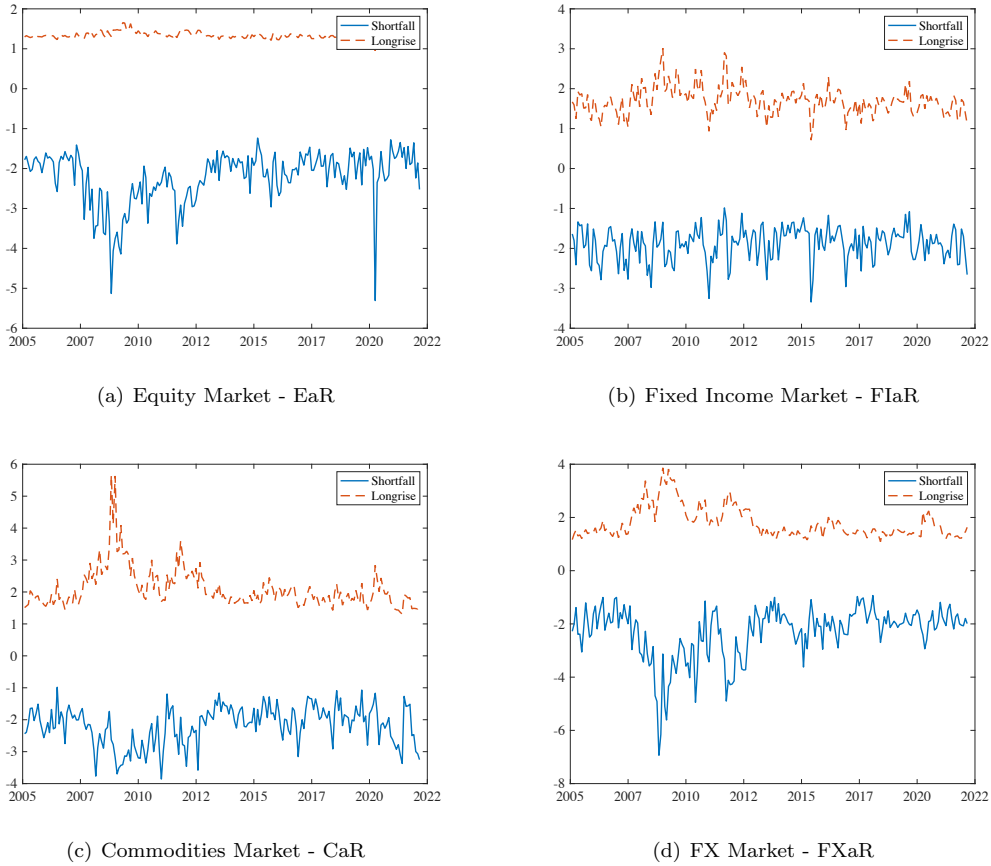
$$ES_{t+h} = \frac{1}{\pi} \int_0^{\pi} \hat{F}_{r_{t+h}}^{-1}(\tau | x_t) d\tau = CVaR_{t+h}$$

$$EL_{t+h} = \frac{1}{\pi} \int_{1-\pi}^1 \hat{F}_{r_{t+h}}^{-1}(\tau | x_t) d\tau$$

While upside and downside relative entropy measures the tail behaviour of the conditional distribution in excess of the tail behaviour exhibited by the unconditional distribution. The expected shortfall and longrise we construct will summarise the lower/upper tail behaviour of the predictive conditional distribution of returns for each one of the considered asset classes in absolute terms.

Therefore, *figure 8* shows the plots of the corresponding time series where the dashed red line is the expected longrise and the solid blue line describes the conditional value-at-risk for each financial asset class. We name the $CVaR_t$ time series Equity-at-Risk (EaR), Fixed Income-at-Risk (FIaR), Commodities-at-Risk (CaR) and Foreign Exchange-at-Risk (FXaR) for the corresponding financial asset class.

Figure 8: Asset Returns Expected Shortfall and Longrise over Time with $\pi = 5\%$



Remarks: This figure displays the evolution over time of the 5 percent expected shortfall ES_t as long as the 95 percent expected longrise EL_t .

Figure 8 validates the intuition and evidence we have so far. Panel (a) emphasises the non-Gaussian properties of the predictive conditional density for the equity market. The left tail of the distribution varies substantially while the upper tail of the distribution is stable. This is consistent with the results that we exhibited in previous sections, that is only on the left tail the predictive density for the stock market varies. Then, panel (b) shows that predictive densities for the fixed income market have stable left and right-hand-side tails. This can be explained by the fact that the time series we are considering to characterise the bond market has almost no tail events, and since most of the predictive power for this particular market comes from the autoregressive specification, one can argue that is the cause the upper and lower tails of the distributions to be stable over time. Then, panel (c) approves the conclusion

we made for the commodities market looking at its upside and downside relative entropy, meaning that for this particular market the upside risk matter more than the downside one as it may be due to the countercyclical feature of the commodities market. Finally, panel (d) backs up the evidence that for the FX market, both upside and downside risks matter with both the expected shortfall and longrise that varies across time. This indicates that during the crisis periods the conditional distribution becomes flattered, which is more a manifestation of higher uncertainty on future returns than greater negative tail outcomes.

5 Tails Spillovers

Now that we generated the so-called $CVaR_t$ time series which are Equity-at-Risk (EaR), Fixed Income-at-Risk ($FIaR$), Commodities-at-Risk (CaR) and Foreign Exchange-at-Risk ($FXaR$). We ask ourselves how these time series interact with each other, more precisely, we want to assess how distribution tails affect each other in times of crisis and tranquil episodes, especially in terms of volatility spillovers. For this, we use a framework first developed in [Diebold & Yilmaz \(2009\)](#) to measure the total volatility spillovers that rely on forecast error variance decompositions from a Vector Autoregression (VAR). This framework had two main disadvantages. First, the framework relies on the Cholesky factor of the VAR, which means the results are sensitive to the variables ordering. Second, this framework only considers the total volatility spillovers index, while in order to bring some insights to our empirical investigation, we need to consider the directional spillovers from/to a given asset class.

To avoid this, we use the same formal specification as the augmented volatility spillovers framework introduced in [Diebold & Yilmaz \(2012\)](#) where they use a generalized vector autoregressive (G-VAR) introduced by [Koop et al. \(1996\)](#) and [Pesaran & Shin \(1998\)](#) in which forecast error variance decomposition is invariant to the variable ordering which enables us to introduce the directional volatility spillovers we need. To describe this framework we take a covariance stationary N -variable VAR(p), described as : $x_t = \sum_{i=1}^p \Phi_i x_{t-i} + \varepsilon_t$, where $\varepsilon \sim (0, \Sigma)$ is a vector of independently and identically distributed disturbances. Thus, the $MA(\infty)$ representation of this process is the following :

$$x_t = \sum_{i=0}^{\infty} A_i \varepsilon_{t-i}$$

With A_i being the $N \times N$ coefficient matrices that defined as :

$$A_i = \Phi_1 A_{i-1} + \Phi_2 A_{i-2} + \dots + \Phi_p A_{i-p}$$

with A_0 being an $N \times N$ identity matrix and with $A_i = 0$ for $i < 0$.

This framework uses variance decompositions to decompose the forecast error variances of each variable into parts which are attributable to the various system shocks which enable the assessment of the fraction of the H step-ahead error variance in forecasting x_i that is due to shocks to x_j , with $\forall j \neq i$. Then we define own variance shares as the fractions of the H -step-ahead error variances in forecasting x_i that are due to shocks to x_i , for $i = 1, 2, \dots, N$, and cross variance shares, or spillovers, as the fractions of the H -step-ahead error variances in forecasting x_i that are due to shocks to x_j , for $i, j = 1, 2, \dots, N$, such that $i \neq j$.

We denote $\theta_{ij}^g(H)$ the H -step-ahead forecast error variance decompositions with $H = 1, 2, \dots, N$. Then $\theta_{ij}^g(H)$ can be formalised as follows:

$$\theta_{ij}^g(H) = \frac{\sigma_{jj}^{-1} \sum_{h=0}^{H-1} (e_i' A_h \Sigma e_j)^2}{\sum_{h=0}^{H-1} (e_i' A_h \Sigma A_h' e_i)}$$

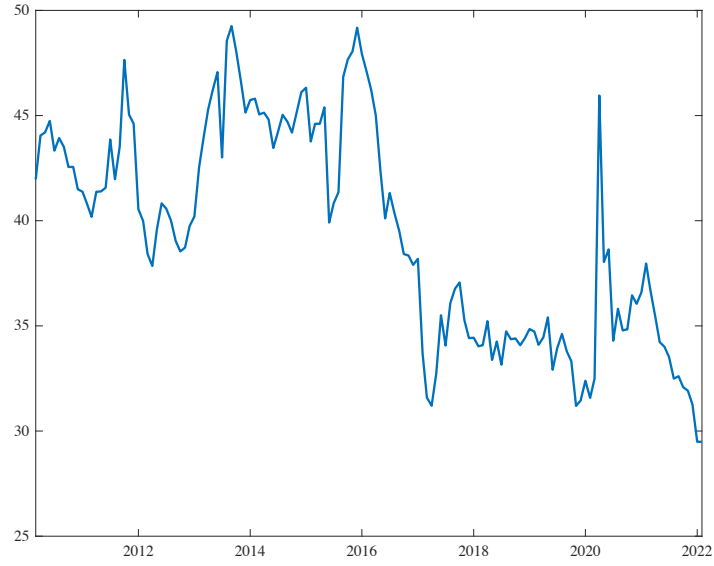
where Σ is the variance matrix for the error vector ε , σ_{jj} is the standard deviation of the error term for the j^{th} equation, and e_i is the selection vector, with one as the i^{th} element and zeros otherwise.

As $\sum_{j=1}^N \theta_{ij}^g(H) \neq 1$ (see [Diebold & Yilmaz \(2012\)](#) for an in-depth explanation), it is necessary to normalize each entry of the variance decomposition matrix by the row sum. We note this adjusted variance share $\tilde{\theta}_{ij}^g(H)$ and define it formally as follows :

$$\tilde{\theta}_{ij}^g(H) = \frac{\theta_{ij}^g(H)}{\sum_{j=1}^N \theta_{ij}^g(H)}$$

This transformation is necessary to extract the information available in the variance decomposition matrix. Then by definition : $\sum_{j=1}^N \tilde{\theta}_{ij}^g(H) = 1$ and $\sum_{i,j=1}^N \tilde{\theta}_{ij}^g(H) = N$

Figure 9: Total left-tail spillovers, Four Asset Classes



Remarks: This figure shows the total spillovers index for the *CVaR* measure of each financial asset class

Table 1: Downside risk spillover index VS CISS

	<i>Dependent variable: Total Downside risk spillover index</i>			
	(1)	(2)	(3)	(4)
CISS	14.084*** (3.380)			
CISS with one month lag		14.089*** (3.389)		
CISS with one quarter lag			9.868*** (3.505)	
CISS with one semester lag				6.775* (3.594)
const	37.297*** (0.658)	37.277*** (0.661)	37.843*** (0.688)	38.199*** (0.712)
Observations	144	143	141	138
R^2	0.109	0.109	0.054	0.025
Adjusted R^2	0.103	0.103	0.047	0.018
Residual Std. Error	4.937 (df=142)	4.950 (df=141)	5.107 (df=139)	5.194 (df=136)
F Statistic	17.360*** (df=1; 142)	17.282*** (df=1; 141)	7.928*** (df=1; 139)	3.553* (df=1; 136)

Note:

*p<0.1; **p<0.05; ***p<0.01

In this table the $ij - th$ entry is the estimated contribution to the forecast error variance of market i coming from innovations to market j .

Downside Risk Spillover

	Stocks	Bonds	Commodities	FX	Directional_FROM_others
Stocks	69.5417	0.48845	1.458	28.5119	30.4583
Bonds	0.13502	96.2586	2.7763	0.83014	3.7414
Commodities	15.589	1.8447	62.8081	19.7582	37.1919
FX	34.7951	0.40868	5.4181	59.3781	40.6219
Directional TO others	50.5191	2.7418	9.6524	49.1003	Downside risk spillover
Directional including own	120.0607	99.0004	72.4605	108.4783	index 28.02%

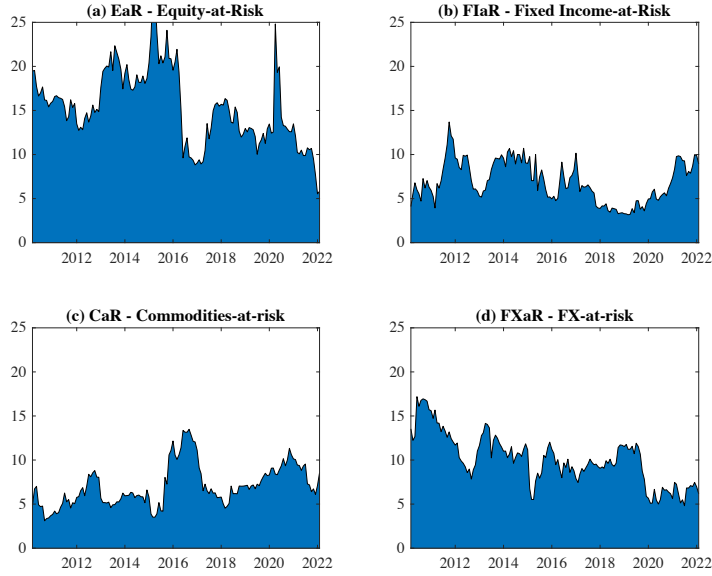
5.1 Gross Directional Tail Risk Spillovers

Using the generalized VAR approach, we can formalise the direction of tail risk spillovers across all asset classes. As the generalized impulse responses and variance decompositions are invariant to the ordering of variables, we calculate the directional spillovers using the normalized elements of the generalized variance decomposition matrix we just defined above. We measure the directional tail risk spillovers received by market i from all other markets j as:

$$S_{i.}^g(H) = \frac{\sum_{\substack{j=1 \\ j \neq i}}^N \tilde{\theta}_{ij}^g(H)}{\sum_{i,j=1}^N \tilde{\theta}_{ij}^g(H)} \times 100 = \frac{\sum_{\substack{j=1 \\ j \neq i}}^N \tilde{\theta}_{ij}^g(H)}{N} \times 100$$

Figure 10 plots the directional tail risk spillovers from each of the four asset classes to others. We notice that those spillovers are fairly volatile and display a surprising smooth cyclical pattern but display very high values of tail risk spillovers. Indeed, during non-crisis periods, the tail risk spillovers from each asset class are about 5 to 10%, but at volatile times those directional tail spillovers increase to close to 15% even 25% for the equity-at-risk. This is crucial evidence of a high tail dependence in the European financial markets.

Figure 10: Directional tail spillovers, FROM four asset classes



Surprisingly, the gross directional tail risk from the fixed income-at-risk is the lowest among the four asset classes we are considering. This highlights that tail events in the equity market have very large repercussions on the other financial markets in the shape of higher volatility of their tails. Then, the bond market has little effect on tail events in other markets.

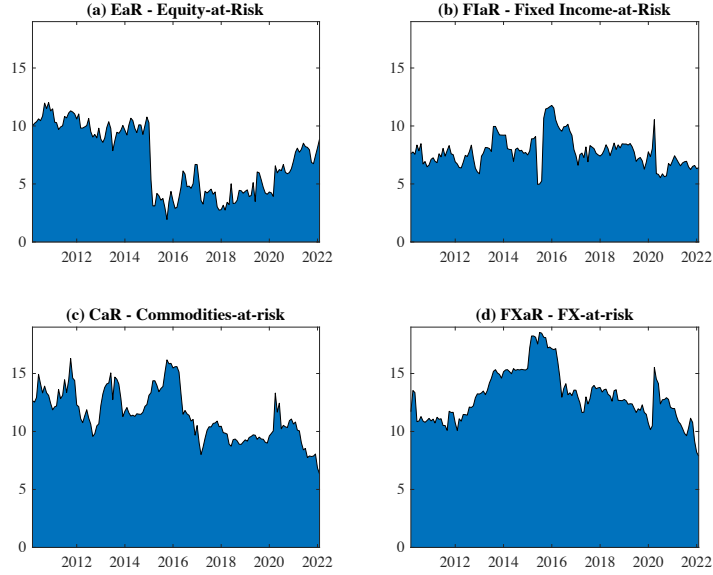
Another aspect we can consider is directional tail risk spillovers going from an asset class i to all other asset classes j . We note it $S_{.i}^g(H)$ and formalize it as:

$$S_{.i}^g(H) = \frac{\sum_{\substack{j=1 \\ j \neq i}}^N \tilde{\theta}_{ji}^g(H)}{\sum_{i,j=1}^N \tilde{\theta}_{ji}^g(H)} \times 100 = \frac{\sum_{\substack{j=1 \\ j \neq i}}^N \tilde{\theta}_{ji}^g(H)}{N} \times 100$$

Figure 11 exhibits the directional tail risk spillovers from the other asset classes for every considered financial market. The overall picture is backwards to the one we described for figure 10. The stock market receives less tail risk directional spillovers from the other market. While the commodities and FX markets receive roughly the same amount of tail risk spillovers and exhibit a declining pattern over time. Meanwhile, the fixed income market reserves very high amounts of spillovers, with a steep increase from

early 2012 to late 2016.

Figure 11: Directional Tail Risk Spillovers, TO four asset classes



5.2 Net Directional Tail Risk Spillovers

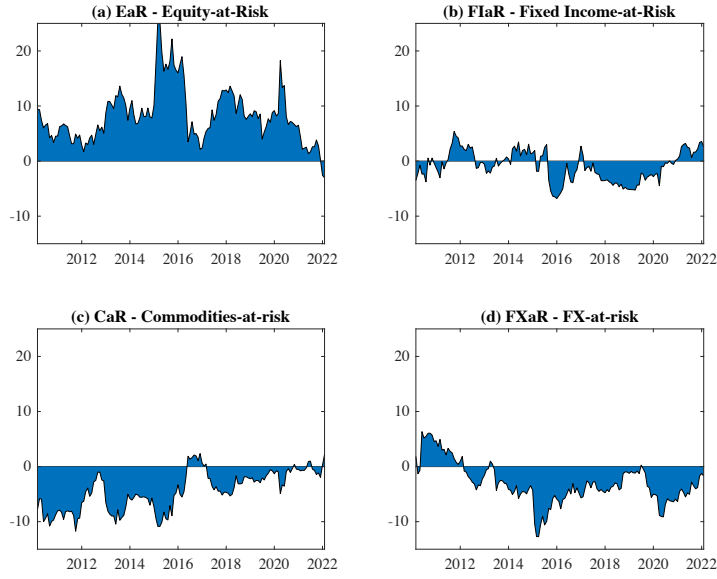
Here, we think about the net tail risk spillovers that give summary information about how much tail outcomes in a given market contribute to the tail events in other markets. It can then be defined as the difference between the gross tail shocks transmitted to and those received from all other markets. We note it $S_i^g(H)$ from market i to all other markets j as :

$$S_i^g(H) = S_i^g(H) - S_i^g(H)$$

Figure 12 plots the net tail risk spillovers for each asset class. We see a coherent picture with the results highlighted by the gross directional tail risk spillovers. First, the stock market is a net spillover giver. It shows that the equity market has cyclical net spillovers that start at 15% in 2010. This can be due to the Greek and Sovereign debt crisis that created a high volatility episode on the left tail of the equity market. In addition, the period between March 2015 and September 2016 characterised by the Chinese stock market turbulence displays a neutral net tail risk spillover period for the European stock markets with positive net spillover periods for the FX market.

It is worth noting that the net spillovers on the stock market display a decreasing pattern. The last spike was at the beginning of the COVID-19 pandemic in early 2020. Secondly, the Commodities market is a net receiver in the first period after the European Sovereign debt crisis while the fixed income market receives a lot of spillovers starting from 2016. Then, the fixed income market has sizeable negative net spillovers starting from 2015. Then, this level attains -10% in September 2016. Lastly, the FX market shows low levels of net spillovers relative to the other asset classes. This market exhibited three net spillover episodes in our sample period. The first one is a neutral and slightly negative period between 2010 and 2016, followed by a positive net spillover period starting in June 2015 and ending at the early stages of the COVID-19 crisis in February 2020.

Figure 12: Net Tail Risk Spillovers, four asset classes



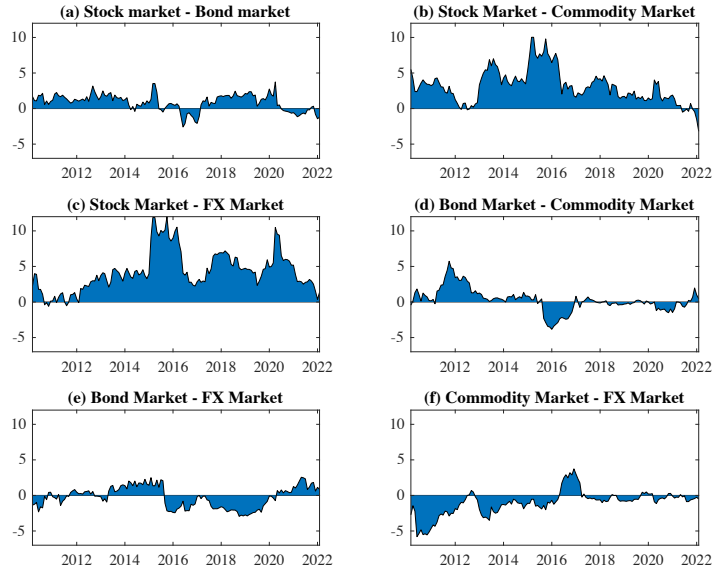
This figure emphasised the high relevance of monitoring the tail risk spillovers that can be induced by the different asset classes. Especially the equity market that seems to have sizeable contagion on the other asset classes. To further investigate the directional tail risk spillovers from one market to the other, we need to build a directional pairwise tail risk spillovers measure.

Therefore, the last measure we take into consideration is the net pairwise tail risk spillovers between our $CVaR$ measures for i and j . It can be defined as the difference between the gross tail innovations transmitted from the asset class i to j and those from j to i . It can then be defined as :

$$\begin{aligned}
 S_{ij}^g(H) &= \left(\frac{\tilde{\theta}_{ji}^g(H)}{\sum_{i,k=1}^N \tilde{\theta}_{ik}^g(H)} - \frac{\tilde{\theta}_{ij}^g(H)}{\sum_{j,k=1}^N \tilde{\theta}_{jk}^g(H)} \right) \times 100 \\
 &= \left(\frac{\tilde{\theta}_{ji}^g(H) - \tilde{\theta}_{ij}^g(H)}{N} \right) \times 100
 \end{aligned}$$

Figure 13 plots the corresponding net pairwise tail risk spillovers. It shows a coherent picture with the measure constructed above and the results displayed in figure 12. First, the equity market has a permanent positive pairwise spillovers index. It means that the market for equities has sizeable repercussions on the other financial markets. There is an exception to this, in panel (b) we see that the net pairwise spillovers between the equity and the commodities market even out starting from 2016. We also see it passing to negative territory in 2021, this can be due to the high pressure on the commodities due to the recovery from the COVID-19 pandemic. Then, in panel (e) we see a period of substantial tail risk spillovers going from the FX to the fixed income market between 2016 and 2020. This result puts more emphasis on the importance of monitoring the tail directional spillovers to predict future negative returns or future repercussions due to a crisis or a period of substantial volatility in other markets. It also highlights the high connectedness of the tails of the predictive distributions.

Figure 13: Net Pairwise left-Tail Risk Spillover



6 Conclusion

This paper provides a simple two-stage procedure for the estimation of the left-tail risk spillovers across financial markets. The first step provides indications that systemic risk is not a strong predictor of future tail outcomes in financial markets. The back-test we provide brings evidence that both the conditional and unconditional estimated densities display very strong out-of-sample performance. Moreover, we see that financial markets do not react the same way during periods of crisis. This shows in the shape of the estimated conditional predictive densities.

The second stage brings to light the tail connectedness across financial asset classes and the sizable amounts of tail risk spillovers across markets. This two-stage procedure provides strong empirical evidence of high contagion risk across financial markets due to their tail dependence. Especially tail risk spillovers going from the stock market to the others.

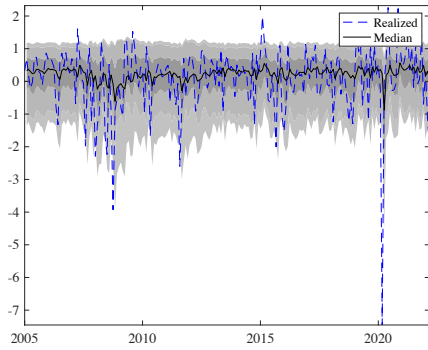
References

- Adrian, T., Boyarchenko, N., & Giannone, D. (2019, April). Vulnerable growth. *American Economic Review*, 109(4), 1263-89. Retrieved from <https://www.aeaweb.org/articles?id=10.1257/aer.20161923> doi: 10.1257/aer.20161923
- Adrian, T., & Brunnermeier, M. K. (2016, July). Covar. *American Economic Review*, 106(7), 1705-41. Retrieved from <https://www.aeaweb.org/articles?id=10.1257/aer.20120555> doi: 10.1257/aer.20120555
- Aikman, D., Bridges, J., Hacıoglu Hoke, S., O'Neill, C., & Raja, A. (2019, September). *Credit, capital and crises: a GDP-at-Risk approach* (Bank of England working papers No. 824). Bank of England. Retrieved from <https://ideas.repec.org/p/boe/boewp/0824.html>
- Azzalini, A., & Capitanio, A. (2003). Distributions generated by perturbation of symmetry with emphasis on a multivariate skew t-distribution. *Journal of the Royal Statistical Society: Series B (Statistical Methodology)*, 65(2), 367-389. Retrieved from <https://rss.onlinelibrary.wiley.com/doi/abs/10.1111/1467-9868.00391> doi: <https://doi.org/10.1111/1467-9868.00391>
- Barro, R. (2006). Rare disasters and asset markets in the twentieth century. *The Quarterly Journal of Economics*, 121(3), 823-866. Retrieved from <https://EconPapers.repec.org/RePEc:oup:qjecon:v:121:y:2006:i:3:p:823-866>.
- Caldara, D., Cascaldi-Garcian, D., Cuba-Borda, P., & Loria, F. (2022, February). *Understanding Growth-at-Risk: A Markov Switching Approach* (Tech. Rep.). Working Paper. Retrieved from https://papers.ssrn.com/sol3/papers.cfm?abstract_id=3992793
- Diebold, F. X., & Yilmaz, K. (2009). Measuring financial asset return and volatility spillovers, with application to global equity markets*. *The Economic Journal*, 119(534), 158-171. Retrieved from <https://onlinelibrary.wiley.com/doi/abs/10.1111/j.1468-0297.2008.02208.x> doi: <https://doi.org/10.1111/j.1468-0297.2008.02208.x>
- Diebold, F. X., & Yilmaz, K. (2012). Better to give than to receive: Predictive directional measurement of volatility spillovers. *International Journal of Forecasting*, 28(1), 57-66. Retrieved from <https://www.sciencedirect.com/science/article/pii/S016920701100032X> (Special Section 1: The Predictability of Financial Markets Special Section 2: Credit Risk Modelling and Forecasting) doi: <https://doi.org/10.1016/j.ijforecast.2011.02.006>
- Engle, R. F. (1982). Autoregressive conditional heteroscedasticity with estimates of the variance of united kingdom inflation. *Econometrica*, 50(4), 987-1007. Retrieved 2024-03-04, from <http://www.jstor.org/stable/1912773>
- Engle, R. F., & Manganelli, S. (1999, October). *CAViaR: Conditional Autoregressive Value at Risk by Regression Quantiles* (University of California at San Diego, Economics Working Paper Series No. qt06m3d6nv). Department of Economics, UC San Diego. Retrieved from <https://ideas.repec.org/p/cdl/ucsdec/qt06m3d6nv.html>
- Ferrara, L., Mogliani, M., & Sahuc, J.-G. (2020, November). *High-frequency monitoring of growth-at-risk* (CAMA Working Papers No. 2020-97). Centre for Applied Macroeconomic Analysis, Crawford School of Public Policy, The Australian National University. Retrieved from <https://ideas.repec.org/p/een/camaaa/2020-97.html>
- Figueres, J. M., & Jarociński, M. (2020, August). *Vulnerable growth in the Euro Area: Measuring the financial conditions* (Working Paper Series No. 2458). European Central Bank. Retrieved from <https://ideas.repec.org/p/ecb/ecbwps/20202458.html>
- Gabaix, X. (2012, 03). Variable Rare Disasters: An Exactly Solved Framework for Ten Puzzles in Macro-Finance *. *The Quarterly Journal of Economics*, 127(2), 645-700. Retrieved from <https://doi.org/10.1093/qje/qjs001> doi: 10.1093/qje/qjs001
- Koenker, R., & Bassett, G. (1978). Regression quantiles. *Econometrica*, 46(1), 33-50. Retrieved from <http://www.jstor.org/stable/1913643>

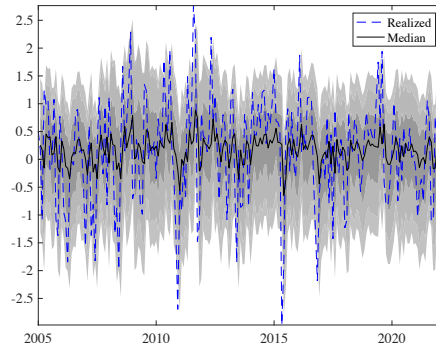
- Koop, G., Pesaran, M. H., & Potter, S. M. (1996, September). Impulse response analysis in nonlinear multivariate models. *Journal of Econometrics*, 74(1), 119-147. Retrieved from <https://ideas.repec.org/a/eee/econom/v74y1996i1p119-147.html>
- Kremer, M., Lo Duca, M., & Holló, D. (2012, March). *CISS - a composite indicator of systemic stress in the financial system* (Working Paper Series No. 1426). European Central Bank. Retrieved from <https://ideas.repec.org/p/ecb/ecbwps/20121426.html>
- López-Salido, J. D., & Loria, F. (2020, February). *Inflation at Risk* (Finance and Economics Discussion Series No. 2020-013). Board of Governors of the Federal Reserve System (U.S.). Retrieved from <https://ideas.repec.org/p/fip/fedgfe/2020-13.html> doi: 10.17016/FEDS.2020.013
- Manganelli, S., White, H., & Kim, T.-H. (2015, June). *VAR for VaR: measuring tail dependence using multivariate regression quantiles* (Working Paper Series No. 1814). European Central Bank. Retrieved from <https://ideas.repec.org/p/ecb/ecbwps/20151814.html>
- Markowitz, H. (1952). Portfolio selection. *The Journal of Finance*, 7(1), 77-91. Retrieved 2024-03-04, from <http://www.jstor.org/stable/2975974>
- Pesaran, M., & Shin, Y. (1998). Generalized impulse response analysis in linear multivariate models. *Economics Letters*, 58(1), 17-29. Retrieved from <https://EconPapers.repec.org/RePEc:eee:ecolet:v:58:y:1998:i:1:p:17-29>
- Rietz, T. A. (1988). The equity risk premium a solution. *Journal of Monetary Economics*, 22(1), 117-131. Retrieved from <https://EconPapers.repec.org/RePEc:eee:moneco:v:22:y:1988:i:1:p:117-131>
- Rossi, B., & Sekhposyan, T. (2014, January). *Alternative tests for correct specification of conditional predictive densities* (Economics Working Papers No. 1416). Department of Economics and Business, Universitat Pompeu Fabra. Retrieved from <https://ideas.repec.org/p/upf/upfgen/1416.html>
- Tsai, J., & Wachter, J. A. (2015). Disaster risk and its implications for asset pricing. *Annual Review of Financial Economics*, 7(1), 219-252. Retrieved from <https://EconPapers.repec.org/RePEc:anr:refeco:v:7:y:2015:p:219-252>

A Appendix A.1

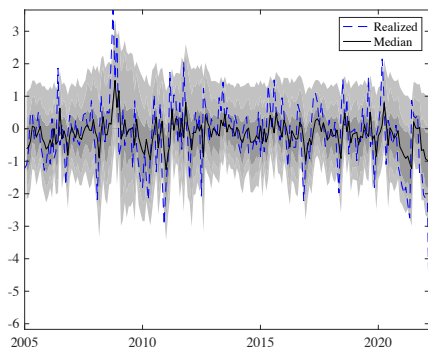
Figure 14: One-month-ahead Predicted Distributions



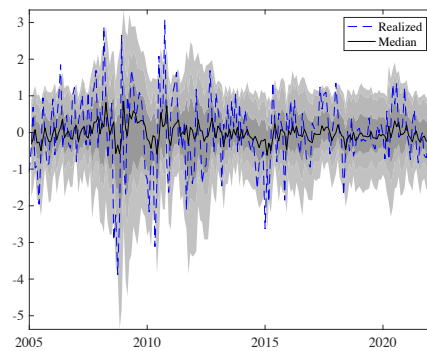
(a) Equity Market



(b) Fixed Income Market



(c) Commodities Market

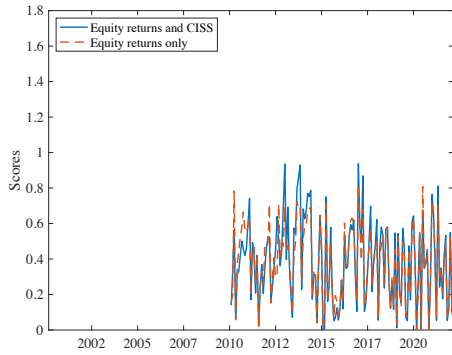


(d) FX Market

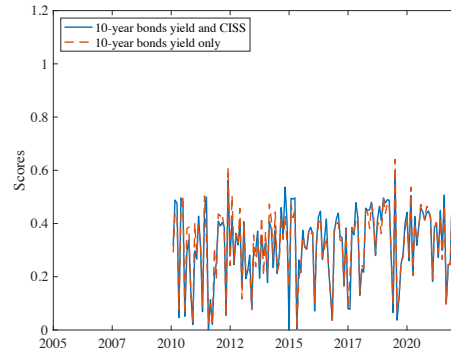
Remarks: INSERT REMARKS HERE.

B Appendix A.2

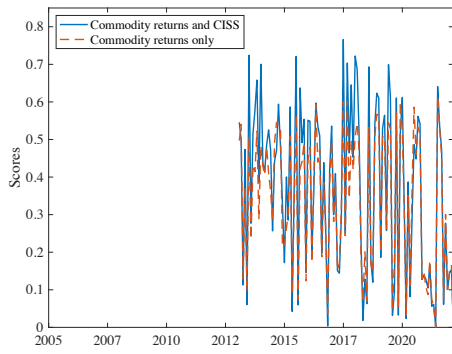
Figure 15: Predictive scores



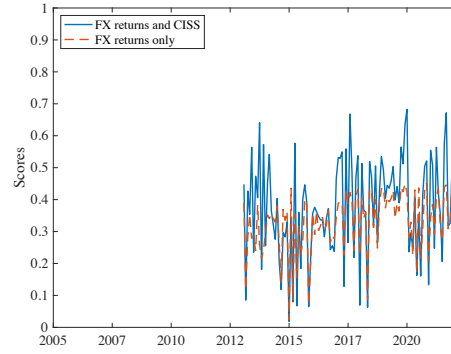
(a) Equity Market



(b) Fixed-Income Market



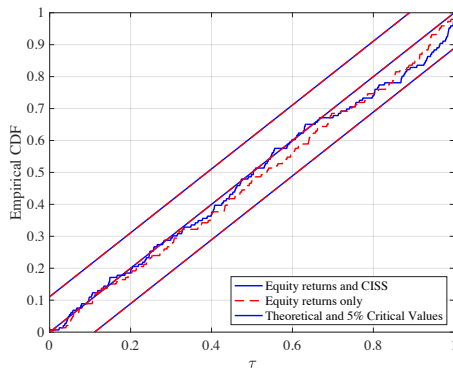
(c) Commodities Market



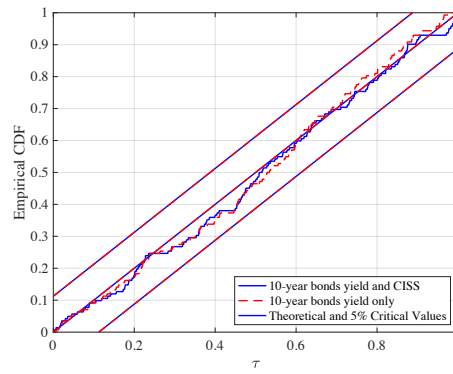
(d) FX Market

Remarks: INSERT REMARKS HERE.

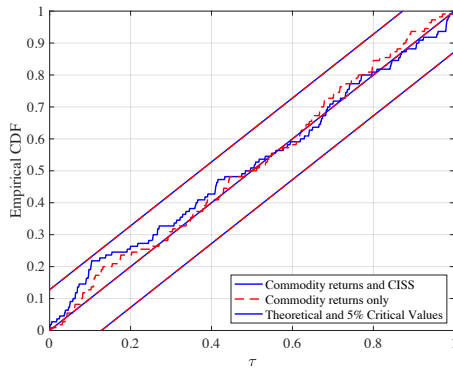
Figure 16: Scores of the Predictive Distributions



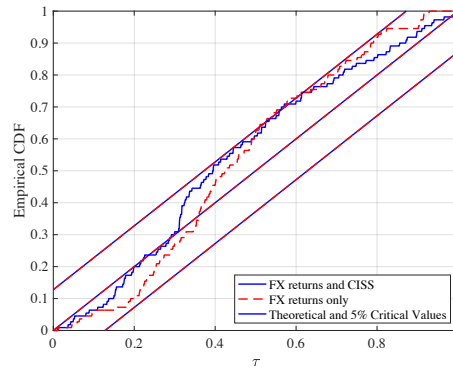
(a) Equity Market



(b) Fixed Income Market



(c) Commodities Market



(d) FX Market

Remarks: INSERT REMARKS HERE.